Received: 21 September 2017 | Revised: 22 October 2017 | Accepted: 23 October 2017

DOI: 10.1002/aoc.4184

FULL PAPER

WILEY Applied Organometallic Chemistry

Crystal structure of *meso*-substituted pyrazolyl porphyrin complexes and their highly active catalyst for oxidation of alkylbenzenes

Yahong Yao[1,2†] | Yanxia Du[1†] | Jun Li[1] | Chen Wang[3] | Zengqi Zhang[1] | Xin Zhao[1]

[1]Key Laboratory of Synthetic and Natural Functional Molecule Chemistry of Ministry of Education, College of Chemistry & Materials Science, Northwest University Xi'an, Shaanxi 710069, People's Republic of China

[2]College of Science, Xi'an University of Architecture and Technology Xi'an, Shaanxi 710055, People's Republic of China

[3]School of Chemical Engineering, Northwest University, Xi'an, Shanxi 710069, People's Republic of China

Correspondence
Jun Li, Key Laboratory of Synthetic and Natural Functional Molecule Chemistry of Ministry of Education, College of Chemistry & Materials Science, Northwest University Xi'an, Shaanxi 710069, People's Republic of China.
Email: junli@nwu.edu.cn

Funding information
National Natural Science Foundation of China, Grant/Award Number: 21671158

During the past few years, a great deal of effort has been devoted to the anchoring of catalytic oxidation. In this work, three new catalysts CuPp, MnPp and ZnPp by solvothermal methods with 5, 10, 15, 20-tetrakis(4-N-pyrazolyl)-phenyl porphyrin (H_2Pp) and the corresponding metal salts have been synthesized and structurally characterized. The single crystal structures determined by X-ray diffraction show the bond distances of M-N in porphyrin cores determined the conformation of porphyrin rings. We explored the catalytic activity of CoPp, CuPp, MnPp and ZnPp for oxidation of alkylbenzenes. The experimental results display these products exhibit high catalytic activities and selectivities for oxidation of ethylbenzene to acetophenone, and can be reused by filtration without appreciable decrease in catalytic activity and selectivity.

KEYWORDS
catalysis, crystal structure, metalloporphyrin, oxidation of alkylbenzene, porphyrin

1 | INTRODUCTION

Porphyrin and metalloporphyrin molecules with unique electronic structures and chemical properties have been extensively exploited as platforms for the study of synthetic and potential application in a wide variety of fields such as chemistry, physics, material science, engineering, biology, and medicine.[1–5] Porphyrin as a typical functional discotic molecule can be easily modified by peripheral substituents or insertion of metal ion into the porphyrin ring.[6,7] Accordingly, they have been widely explored as the building blocks for the construction of diverse functional materials, such as photonic devices conductive polymers, chemical sensors, receptors for selective catalysis, material for magnetic ordering, and light-harvesting materials, [8–13] especially as catalyst, a variety of metalloporphyrins with different substituent groups were synthesized and showed excellent catalytic properties.[14–18] The first oxidation system with synthetic metalloporphyrin as a catalyst was developed by Groves and co-workers in 1979.[19] Subsequently, numerous reports on metalloporphyrin-catalyzed oxidation systems have appeared in the literature, as described in previous reviews.[20–23]

Metal-catalyzed selective oxidation of organic substrates under mild conditions, with dioxygen, air or tert-

†These authors contributed equally to this work.

 Copyright © 2017 John Wiley & Sons, Ltd.

butylhydroperoxide as the sole terminal oxidant, is an economic and green methodology for the synthesis of epoxides, alcohols, ketones, and aldehydes.[24] Furthermore, the catalytic functionalities of the metalloporphyrins can be easily achieved by modulating catalytic-active metal sites and tailoring the peripheral environments of metalloporphyrins. Design different porphyrins and metalloporphyrins provide a new strategy for seeking novel functional to catalyst. However, over the last few decades, many catalyst of porphyrins or metalloporphyrins have been reported with peripheral substitutes commonly being carboxyl, pyridine or imidazole groups,[25,26] pyrazolyl-functionalized porphyrins and the influence of coordination metal atoms in center of porphyrin ring on catalytic activity have rarely been reported.

Our group has been working on the synthesis of different metalloporphyrin to research these new materials for their heterogeneous biomimetic catalysis over the past several years. In this work, we synthesized and characterized four kinds of catalysts CuPp, MnPp and ZnPp by the ligand 5, 10, 15, 20-tetrakis (4-N-pyrazolyl) phenyl porphyrin (H_2Pp) (Figure 1). We explored the best catalytic conditions for ethylbenzene oxidation to acetophenone, and used the optimal experimental conditions to study the catalytic activity of CoPp, CuPp, MnPp and ZnPp for alkylbenzenes oxidation. MnPp exhibits highly efficient and selective catalytic for alkylbenzenes oxidation.

2 | EXPERIMENTAL DETAILS

2.1 | Materials and methods

All analytical reagents were purchased from commercial sources and used without further purification expect pyrrole N, N-dimethyl formamide (DMF), which was distilled before use. Elemental analyses (C, H and N) were performed by Vario EL-III CHNOS instrument. UV-vis spectra were measured on a Shimadzu UV 1800 UV-vis-NIR spectrophotometer. UV-vis diffuse reflectance spectra (DRS) were recorded on a Shimadzu UV-3100 spectrophotometer by using $BaSO_4$ as a reference. The fluorescence spectrum was recorded at room temperature on a Hitachi F4500 fluorescence spectrofluorometer with a xenon arc lamp as the light source. FT-IR spectra were obtained on a BEQUZNDX-550 spectrometer on samples embedded in KBr pellets. Mass spectrometry (MS) analysis were carried out on a matrix assisted laser desorption/ionization time of flight mass spectrometer (MALDI-TOF MS, Krato Analytical Company of Shimadzu Biotech, Manchester, UK). The X-ray diffraction (XRD) patterns were recorded on a Bruker D8 diffractometer using graphite monochromatic copper radiation (Cu Kα) at 40 kV, 30 mA over the 2θ range from 20° to 80°. The crystallographic data sets were collected on a Bruker SMART CCD diffractometer with graphite monochromated Mo Kα radiation (λ = 0.71073 Å). Thermal Analysis (TGA) experiments were carried out in N_2 at a heating rate of 10 °C·min^{-1} on a NETZSCH STA 449C thermal analyzer instrument.

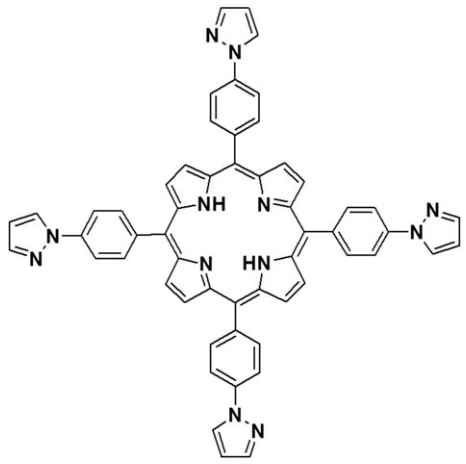


FIGURE 1 Molecule structure of 5, 10, 15, 20-tetrakis(4-N-Pyrazolyl)phenyl porphyrin (H_2Pp)

2.2 | Synthesis

5, 10, 15, 20-tetrakis (4-N-pyrazolyl) phenyl porphyrin (H_2Pp) and CoPp was synthesized and characterized in our previous report.[27]

CuPp: Solvothermal reactions of Cu $(OAc)_2{\cdot}4H_2O$ (7.51 mg, 30 mmol) and H_2Pp (8.72 mg, 10 mmol) were in DMF (5 ml) at 90 °C for 72 hours. After cooling down to room temperature, purple bulk-shaped crystals were obtained. Yield 35.2%; Composition $[Cu(C_{56}H_{36}N_{12})(C_2H_7N)]$). Anal. Calcd for $C_{58}H_{43}CuN_{13}$: C, 68.69; H, 4.42; N, 18.44%; Found: C, 68.68; H, 4.40; N, 18.47%; UV-Vis (DMF) λ_{max}: 428 nm, 549 nm, 604 nm; FT-IR (KBr): v, cm^{-1}, 3331, 2360, 1663, 1505, 1394, 1008, 941.

MnPp: MnPp was prepared from $MnCl_2{\cdot}4H_2O$ (5.94 mg, 30 mmol) and H_2Pp (8.72 mg, 10 mmol) according to the procedures similar to that of compound CuPp. Yield 36.5%. Composition $\{Mn[(C_{56}H_{36}N_{12})(DMF)_2Cl]\}$. Anal. Calcd for $C_{62}H_{50}ClMnN_{14}O_2$: C, 66.85; H, 4.54; N, 17.62%; Found: C, 66.87; H, 4.53; N, 17.61%; UV-Vis (DMF) λ_{max}: 470 nm, 578 nm, 618 nm; FT-IR (KBr): v, cm^{-1}, 3327, 2360, 1646, 1512, 1399, 1002, 937.

ZnPp: ZnPp was also prepared from $Zn(OAc)_2{\cdot}2H_2O$ (5.58 mg, 30 mmol) and H_2Pp (8.72 mg, 10 mmol) according to aforementioned procedures. Yield 43.5%; Composition $[Zn(II)(C_{56}H_{36}N_{12})]$. Anal. Calcd for Zn $[C_{56}H_{36}N_{12}]$: C, 71.37; H, 3.85; N, 17.84%; Found: C, 71.35; H, 3.87; N, 17.84%; UV-Vis (DMF) λ_{max}: 429 nm, 562 nm, 604 nm;

FT-IR (KBr): v, cm^{-1}, 3429, 2349, 1646, 1529, 1394, 1193, 1048, 998, 937.

2.3 | X-ray crystal structure analysis

The crystallographic data of CuPp and MnPp were collected at 296 K by a Bruker SMART CCD diffractometer with graphite monochromated Mo Kα radiation (λ = 0.71073 Å). Absorption corrections were applied using SADABS program.[28] The structures were solved by direct method and refined by full-matrix least-squares techniques using the SHELXL-97 program.[29] Anisotropic thermal parameters were assigned to all non-hydrogen atoms. Hydrogen atoms were placed in geometrically calculated positions. The crystal parameters of CuPp and MnPp are given in Table 1. Selected bond distances and angles are listed in Table S1.

2.4 | Catalytic oxidation procedure

All the oxidation reactions were carried out in a sealed vial. A mixture of alkylbenzenes (1 m mol), tert-butylhydroperoxide (TBHP, 0.8 mmol), catalyst (0.005 mmol) and H_2O (1.5 ml) was stirred at 80 °C for 20 h. when time up, the identity of the products was determined by gas-chromatography (GC), compared with the authentic samples analyzed under the same conditions. The yield of products was also obtained by GC analysis with a flame-ionization detector (FID) using a capillary SE-54 column.

TABLE 1 The crystal parameters of CuPp and MnPp

Compounds	CuPp	MnPp
Empirical formula	$C_{58}H_{43}CuN_{13}$	$C_{62}H_{50}ClMnN_{14}O_2$
Formular weight	985.59	1113.55
Wavelength(Å)	0.71073	0.71073
θ range (°)	2.47-25.10	1.22-25.04
Crystal system	Triclinic	Tetragonal
Crystal size(mm)	0.24 × 0.21× 0.16	0.26 × 0.21 × 0.17
T (K)	296(2)	296(2)
Space group	*P-1*	*P4(3)*
a (Å)	10.737(3)	16.654(6)
b (Å)	15.388(4)	16.654(6)
c (Å)	16.730(4)	19.517(7)
α (°)	102.176(5)	90
β(°)	93.409(5)	90
γ (°)	90.779(5)	90
V ($Å^3$)	2696.2(12)	5413(4)
Z	2	4
Dcalc ((mg/m^3)	1.24	1.366
F(0 0 0)	1022	2312
μ(mm^{-1})	0.455	0.353
R_1, wR_2 [I >2σ(*I*)]	0.0972, 0.2802	0.0721, 0.2027
R_1, wR_2 (all data)	0.1658,0.3392	0.0979, 0.2345
Goof(F^2)	1.029	1.044

3 | RESULTS AND DISCUSSIONS

3.1 | Crystal structures

CuPp crystallizes in the triclinic system with a space group of *P-1*. The asymmetric unit contains one Cu (II) Pp-complex and one dimethylamine molecule (DMF decomposition) (Figure 2a). The copper atom resides at the center of porphyrin macrocycle. The dihedral angles between the neighboring pyrrole rings are 6.865(230)°,

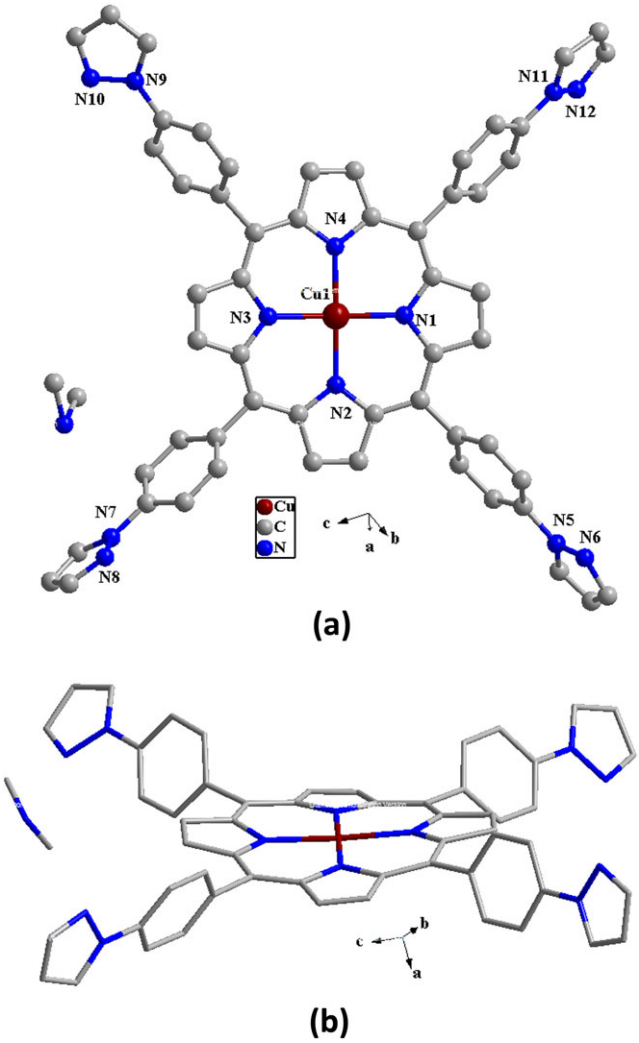


FIGURE 2 **(a)** And (**b**) the coordination environment of cu(II) and structure conformation of CuPp. (the hydrogen atoms are omitted for clarity, cu, red; N, blue; C, gray)

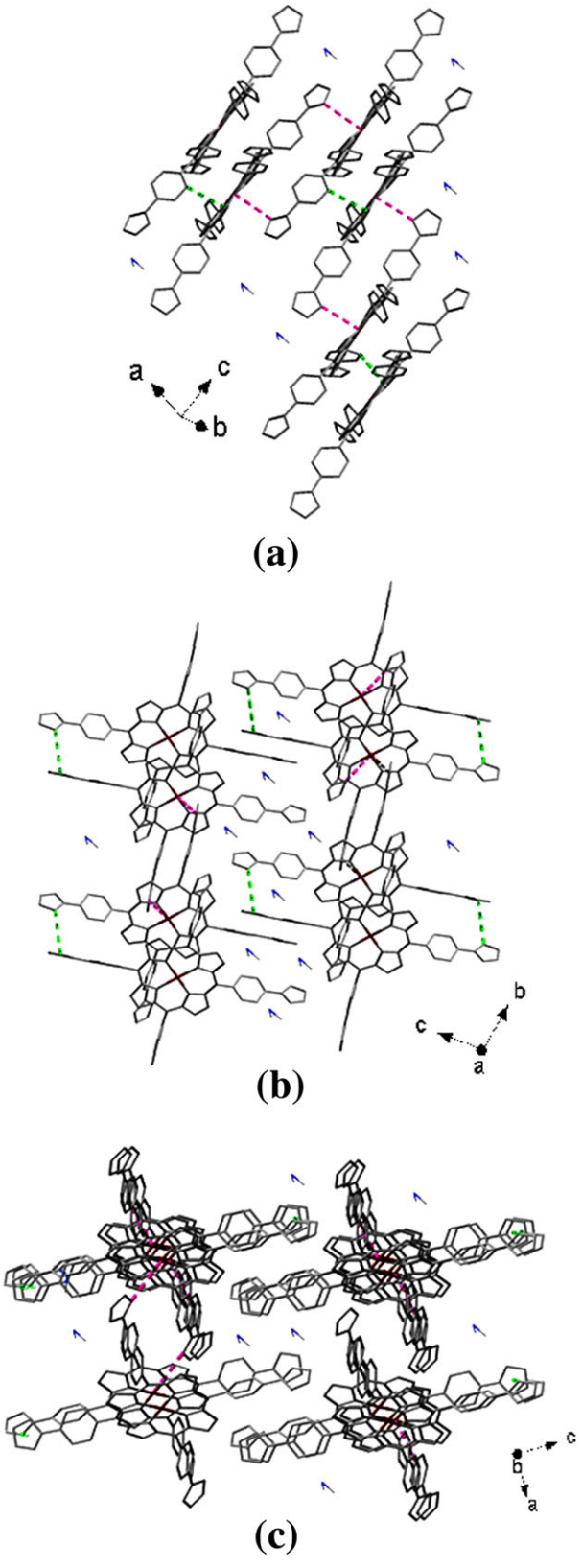


FIGURE 3 **(a)** 1D chains structure of CuPp; **(b)** 2D layers structure of CuPp; **(c)** 3D structure of CuPp. (the hydrogen atoms are omitted for clarity; the C-H···π and π···π interactions are indicated by dotted lines)

4.827(244)°, 13.444(185)° and 11.717(231)°, respectively. The peripheral four substituent groups extend along the porphyrin plane and the angles between the two contrapuntal pyrazolyl are 42.7951(230)° and 35.904(183)°, respectively. The porphyrin macrocycle in CuPp displays a distorted conformation (Figure 2b).

Analysis of the CuPp reveals that phenyl rings and pyrazolyl ring could form weak C-H···π contact as hydrogen donor. C-H···π interactions (Figure S2, green dotted line) between the phenyl C atom and pyrrole rings and the C-H···π (Figure S2, red dotted line) of pyrazole C atom and adjacent porphyrin macrocycles interlink the molecules to form 1D chain structure (Figure 3a). The neighbouring chains connect by π···π interactions (green dashed lines) between the pyrazolyl of two adjacent porphyrin rings to form 2D layer structure (Figure 3b). The layers link each other by π···π interactions between porphyrin macrocycles to construct a 3D structure (Figure 3 c). The distances of C-H···π interactions are in supporting information (Figure S2).

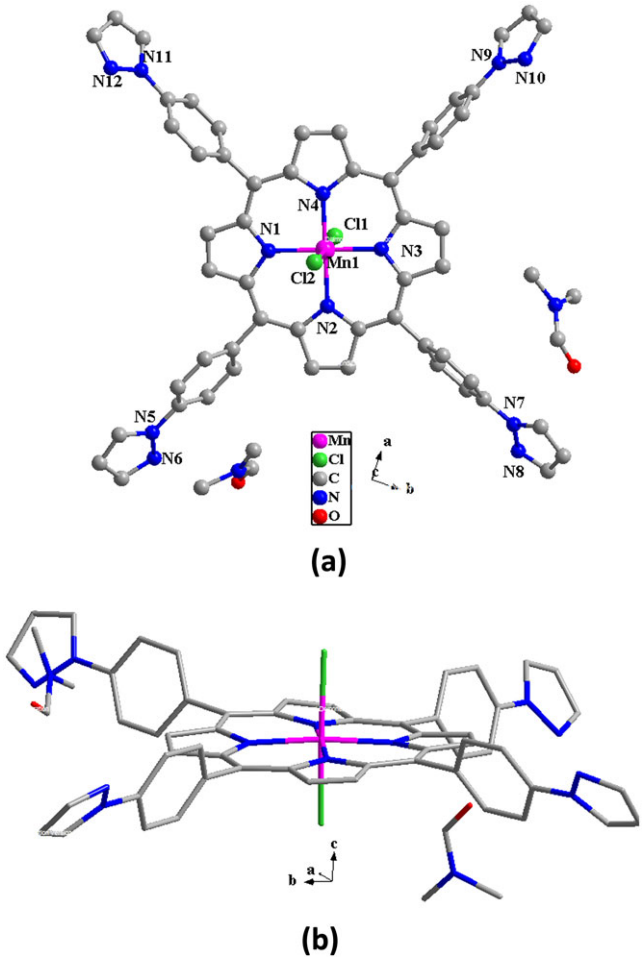


FIGURE 4 **(a)** And (**b**) the coordination environment of Mn(III) and structure conformation of MnPp**.** (the hydrogen atoms are omitted for clarity, Mn, rose; N, blue; C, gray; cl, green)

MnPp crystallizes in the tetragonal system with a space group of *P4 (3)*. The asymmetric unit contains the MnPp-complex and two DMF molecules (Figure 4a). The manganese atom resides at the center of porphyrin macrocycle, two chloric atoms coordinate with the manganese atom and respective accounts for 1/2 of manganese atoms, the manganese atom are trivalent in MnPp. The bond distances from Mn(III) (at the center of a saddle-distorted nonplanar porphyrin macrocycle) to the Cl atoms are 2.385(2) Å and 2.4619(14) Å, respectively. The dihedral angles between the neighboring pyrrole rings are 9.470(133)°, 7.891(146)°, 3.580(148)° and 5.862(107)°, respectively. The peripheral four substituent groups extend along the porphyrin plane and the angles between the two contrapuntal pyrazolyl are 47.363(282)° and 32.214(396)°, respectively. The porphyrin macrocycle in MnPp displays a little distorted conformation (Figure 4b).

In the structure of MnPp, there are two kinds of C-H··π interactions and two kinds of hydrogen bonds. The C-H···π interactions are: the pyrazolyl C atom and adjacent porphyrin macrocycle and the hydrogen bonds are Cl-C···H bonds and Cl-O···H bonds to construct a 3D structure (Figure 5).

The bond distances from M (at the center of a distorted nonplanar porphyrin macrocycle) to pyrrole N are Cu-N(1) 1.995(5) Å, Cu-N(2) 1.979(6) Å, Cu-N(3) 1.993(6) Å, Cu-N(4) 1.996(6) Å in CuPp and Mn-N(2) 2.013(2) Å, Mn-N(4) 2.014(2) Å, Mn-N(3) 2.020(2) Å, Mn-N(1) 2.021(2) Å in MnPp, respectively. This is different from the literature,[27] the Co–N bond distances are

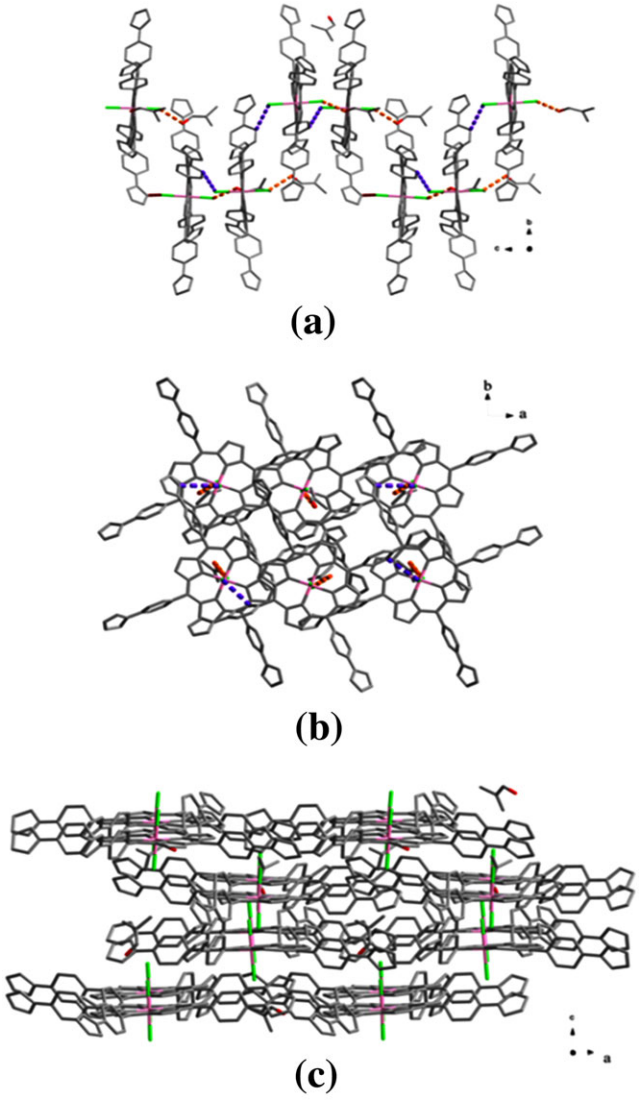


FIGURE 5 **(a)** 1D chains structure of **MnPp** (**b**) 2D layers structure of **MnPp**; (**c**) 3D structure of **MnPp**. (the hydrogen atoms are omitted for clarity; the C-H···π interactions are indicated by dotted line)

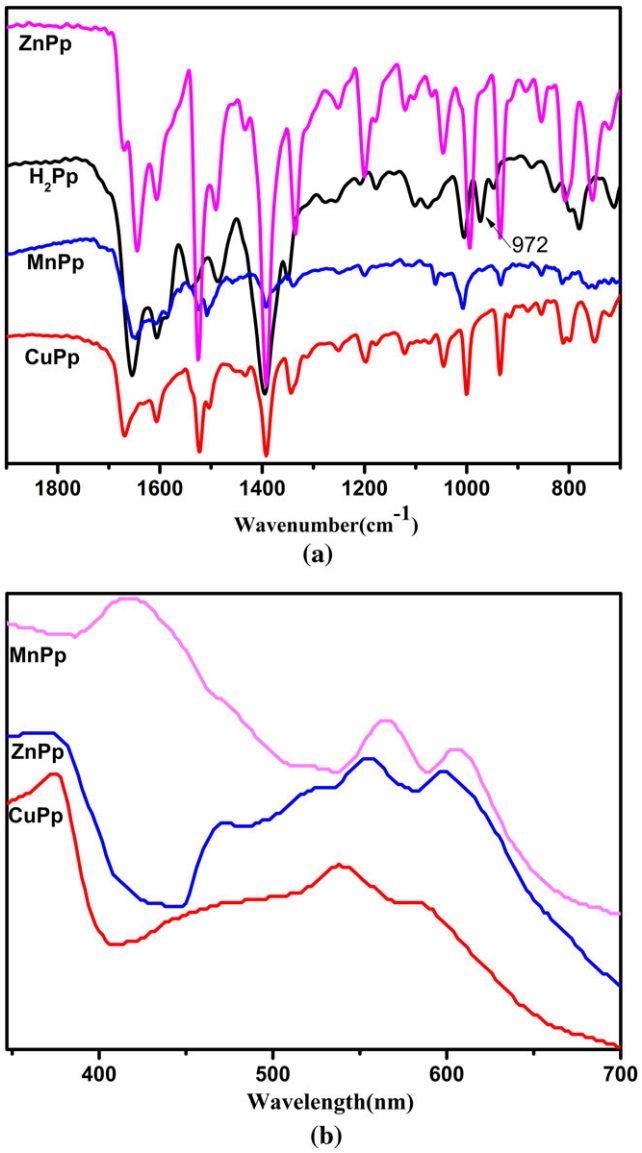


FIGURE 6 **(a)** And **(b)** are the FT- IR and UV–vis spectras of CuPp, MnPp and ZnPp in solid

Co-N(1) 1.938(9) Å, Co-N(2) 1.946(8) Å, Co-N(3) 1.950(9) Å, Co-N(4) 1.948(9) Å in CoPp which are significant difference, and the angles between the two contrapuntal pyrazolyl are 31.499(221) ° and 77.327(207) °, respectively. Furthermore different size of Cu(II), Co(II) and Mn(III) metal at the center of porphyrin macrocycle make different the coordination model between metal ions and N atoms, and then lead to change in geometry of the porphyrin molecule. The porphyrin macrocycle in MnPp and CuPp displays a little distorted conformation due to the size of copper (II) and manganese (III) ions and similar M–N distances. However, the smaller size of the cobalt ion causes a considerable saddle-type deformation of the porphyrin ring in order to accommodate the shorter Co–N coordination bonds. In the literature,[30] the Co–N bond distances is range from 1.802(6)-1.987(5) Å, the porphyrin macrocycle is close to a perfect plane.

3.2 | Thermogravimetric and X-ray power diffraction (PXRD) analysis

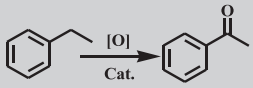
Thermogravimetric analysis (TGA) was taken to examine the thermal stability of the compounds. As can be seen in Figure S4, a weight loss of the CuPp and MnPp from 25 °C to 300 °C should be attributed to solvent molecules. With the temperature increased, the curve is followed by a steady platform up to 427 °C; after this, the network starts to decompose. However, ZnPp exhibits a relatively steady plateau up to 426 °C before decomposition of the network. So that stable state can be maintained for the CuPp and MnPp below 427 °C, and for the ZnPp below 426 °C.

The phase purity of CuPp, MnPp and ZnPp were verified by powder X-ray diffraction studies, which have revealed that the diffraction patterns of the fresh samples are consistent with the simulated ones (Figure S5).

3.3 | The FT- IR spectra and solid-state UV–vis spectra

The FT- IR spectra of CuPp, MnPp and ZnPp showed similar characters (Figure 6a), and a new band appeared around 1000 cm^{-1} was assigned to M-N vibration, while δ(NH) of the porphyrin ring bands at 972 cm^{-1} were absent in compounds CuPp, MnPp and ZnPp. The bands ascribed to the stretching vibration of –C=N– at 1654, 1669, 1650 and 1645 cm^{-1} were observed in the IR spectra of H_2Pp, CuPp, MnPp and ZnPp respectively. The UV–vis spectra of CuPp, MnPp and ZnPp were examined in the

TABLE 2 Selective oxidation of ethylbenzene catalyzed by MnPp



Entry	Catalyst[a]	T(°C)	[O]	Solvent[b]	Yields(%)[c]	Selectivity(%)[d]
1	CoPp	80	TBHP	H_2O	88	>99
2	CuPp	80	TBHP	H_2O	79	>99
3	ZnPp	80	TBHP	H_2O	56	>95
4	MnPp	80	TBHP	H_2O	99	>99
5	H_2Pp1	80	TBHP	H_2O	27	>90
6	Blank	80	TBHP	H_2O	6	>78
7	MnPp	65	TBHP	CH_3CN	83	>99
8	MnPp	80	TBHP	CH_3CN	82	>99
9	Blank	65	TBHP	CH_3CN	5	>78
10	MnPp	65	TBHP	H_2O	70	>99
11	MnPp	80	H_2O_2	H_2O	70	>99
12	Blank	80	H_2O_2	H_2O	4	>78

Conditions:

[a]mixture of catalyst (0.005 mmol), ethylbenzene (0.05 mmol), and oxidant (0.5 mmol);

[b]2.5 ml solvents;

[c]Based on GC analysis;

[d]Selective oxidation of ethylbenzene to acetophenone

solid state (Figure 6b) at room temperature. The UV–vis spectrum of CuPp is characterized by a Soret band at 364 nm and only one Q band at 539 nm, there are one Soret band at 456 nm and 370 nm, two Q bands at 574-614 nm and 554-599 nm for MnPp and ZnPp, respectively. The decreased number of Q bands in the spectra of metalloporphyrins is owing to the symmetry increase of porphyrin ring after metal ions coordinating with the N atoms of porphyrin. The delocalized π bonds of ZnPp and CuPp decreased the average electron density of the porphyrin, which increased the energy for electron transition, leading to a blue shift in the Soret band. Furthermore Mn(III) ion insertion into the free-base porphyrin elicited a large bathochromic shift of the Soret band compared with H_2Pp (Soret band at 390 nm and four Q band at 513-644 nm), which might be attributed the charge transfer between the $a_{1u}(\pi)$ and $a_{2u}(\pi)$ orbital of the porphyrin ring to the $e_g(d\pi)$ orbitals of manganese (III) center metal.[31,32]

3.4 | Catalytic properties

3.4.1 | Conditions optimization

The optimal reaction conditions for ethylbenzene catalysis were investigated by the influences of reaction temperature, oxidant and solvent according to prior reports in the literature.[33,34] A series of experiments was carried out by choosing MnPp as catalyst, with the model test for ethylbenzene oxidization. Blank experiments in the absence of catalyst were carried out for easy comparison. Table 2 are summarized the results catalyzed, it was obvious that four metalloporphyrins display much higher catalytic activity than the molecular H_2Pp catalyst for the oxidation of ethylbenzene. The yield of acetophenone in solvent of CH_3CN with 83% conversion (Table 2, entry 7) were higher than that of in solvent of H_2O (Table 2, entry 10) at 65 °C. However, the activity was remarkably improved in the solvent of H_2O and almost the same in solvent of CH_3CN when the temperature rose to 80 °C, corresponding to 99% and 82% conversion, (Table 2, entry 4 and 8) respectively. Furthermore, for a better understanding of the role of oxidant on the catalytic reaction, different oxidant was investigated in solvent of H_2O at 80 °C (Table 2, entry 4 and 11). The use of TBHP leads to significantly higher yields compared with H_2O_2. From these experiments, the optimal reaction conditions for ethylbenzene oxidation to acetophenone was in solvent of H_2O at 80 °C using tert-butylhydroperoxide (TBHP) as the oxidant. Compare with the reported literature,[35] the yield of acetophenone was increased by 22% in such condition.

To shed further light on the catalytic activities, time-dependent experiments were also carried out at different time (within 30 hours). Figure 7a was the time-yield plot for the oxidation of ethylbenzene. It showed that these catalysts exhibited strong catalytic activities. The yield of acetophenone increased sharply at the beginning of 20 hours, and the increasing tendency of yield became leveling off when exceeded 20 hours.

3.4.2 | Catalysts reuse

We assessed the catalytic activities and reuse of CoPp, CuPp, MnPp and ZnPp according to the above selected conditions. The results (Table 2) showed that these catalysts efficiently catalyzed the conversion of ethylbenzene to the only product acetophenone quantitatively in 88%, 79%, 99% and 56% yield, respectively. After reaction finished, solid CoPp CuPp, MnPp and ZnPp was

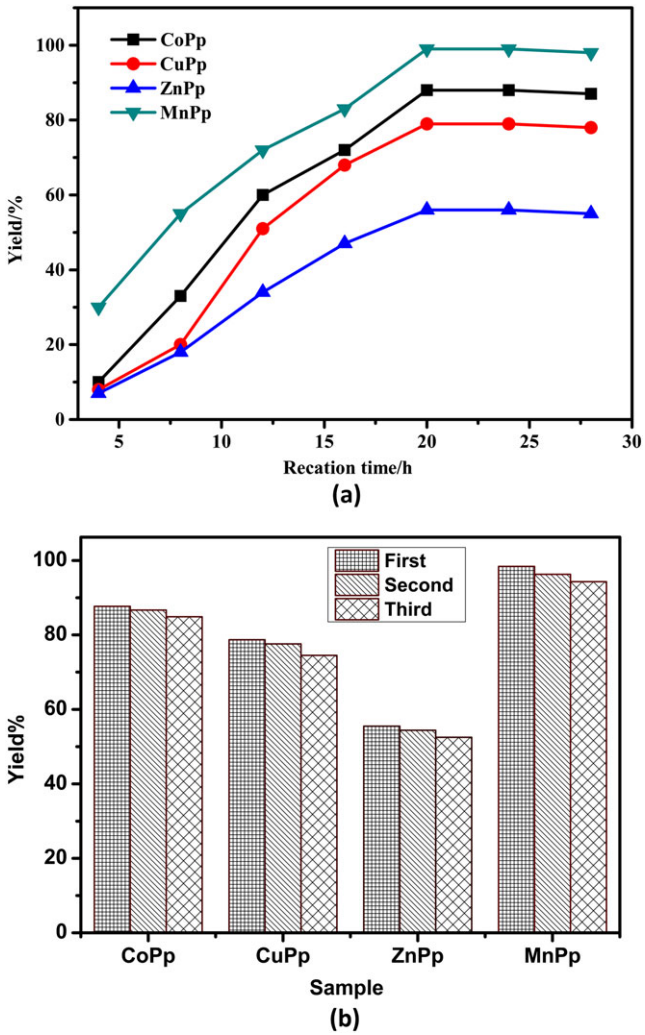
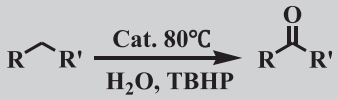
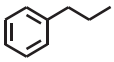
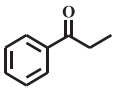
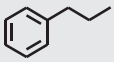
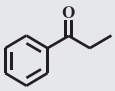
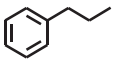
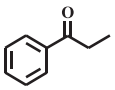
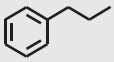
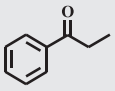
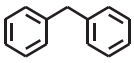
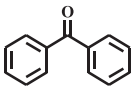
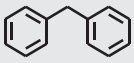
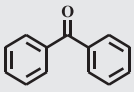
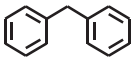
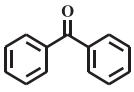
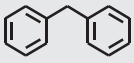
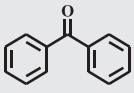


FIGURE 7 **(a)** Time-yield plot for the oxidation of ethylbenzene catalyzed by CoPp, CuPp, MnPp and ZnPp; **(b)** the yield after three cycles. (conditions: The ethylbenzene oxidation was performed in solvent of H_2O at 80 °C using TBHP as the oxidant, yields determined by GC)

TABLE 3 Selective oxidation of alkylbenzenes catalyzed by the four complexes in H_2O



Entry	Substrate	Product	Catalyst	Yields(%)	TON	Selectivity(%)
1			CoPp	86	1720	98
2			CuPp	71	1420	85
3			ZnPp	49	980	82
4			MnPp	91	1820	99
5			CoPp	72	1440	98
6			CuPp	65	1300	99
7			ZnPp	43	860	86
8			MnPp	79	1580	99
9			CoPp	70	1400	99
10			CuPp	61	1220	99
11			ZnPp	38	760	82
12			MnPp	73	1460	99

Conditions: Alkylbenzenes (0.1 mmol), TBHP (0.15 mmol), catalyst (0.005 mmol), H_2O (2.5 ml) were stirred at 80 °C for 20 h. Conversion (%) and selectivity (%) were determined by GC on an SE-54 column.

easily recovered by centrifuging and filtration and subsequently used in successive runs with only slightly decreased in catalytic efficiency. As showed in the Figure 7b, the catalytic activity showed no obvious decreased after three cycles.

3.4.3 | Catalytic oxidation of alkylbenzenes

These complexes catalytic oxidation of alkylbenzenes were examined according to a procedure similar to that for the oxidation of ethylbenzene. GC analysis (Table 3) displayed that the compounds efficiently catalyzed these chemical transformations. MnPp was the highest catalytic activity for alkylbenzenes oxidation, and their selectivity were over 99% indicating the products were almost the only one. The conversion of 1-phenylpropane was as high as 91% which was far more than that of diphenylmethane and 1, 2, 3, 4-tetrahydronaphalene. Followed by CoPp and then CuPp, in which the conversions were slightly decreased but the selectivity was still quite high and maintained more than 98%. However, ZnPp showed low catalytic activity compared to that for MnPp, CoPp and CuPp, which alkylbenzenes oxidation yields for alkylbenzenes reduced to about 40%.

The significant difference of CoPp, CuPp, MnPp and ZnPp for their catalytic transformation of alkylbenzenes to aromaticketones clearly indicated the roles of metal in centre of porphyrin macrocycle as the efficient catalytic sites. It was found that the reactivity of manganese (III) porphyrin catalyst was greatly affected by axial Cl atoms gave the highest catalytic activity in the oxidation of alkylbenzenes. In the process of catalysis, the Cl atom from the longer Mn-Cl bond easy to take off and form transition state (porphyrin)ClMn^{V}(O), to improve the catalytic activity of the catalyst MnPp. Meanwhile, the significant difference of catalytically oxidize various alkylbenzenes of CoPp, CuPp, MnPp and ZnPp was observed under the above-mentioned reaction conditions. For CoPp, CuPp, MnPp and ZnPp, the conversion of substrate decreased gradually when the size of the substrate increases. The much lower catalytic conversion for the larger substrates might be attributed to larger size which they were difficult to access to the interior pores of porphyrin because of steric effect. This study clearly demonstrates that the catalytic oxidation of alkylbenzenes does occur inside the pores of porphyrin.[33]

4 | CONCLUSIONS

In summary, the single crystal structures of CuPp, MnPp and microcrystal ZnPp from the ligand 5, 10, 15, 20-tetrakis(4-N-pyrazolyl)phenyl porphyrin (H_2Pp) were synthesized and characterized. The distances of M-N bonds in center of the porphyrin rings determine the conformation of porphyrin macrocycle. The results of thermogravimetric showed they possessed ideal thermostability. In addition, the higher catalytic efficiency observed for MnPp in comparison with the CoPp, CuPp and ZnPp. These results demonstrated that the metal atoms in center of porphyrin macrocycle determine the catalytic activity of metalloporphyrin, and the catalytic activity order is MnPp>CoPp>CuPp>ZnPp.

ACKNOWLEDGEMENT

This work has been supported by the NNSF (No. 21271148), Scientific Research Program Funded by Shaanxi Provincial Education Department (No. 15JK1736), Natural Science Foundation of Shaanxi province (No. 2014JM2054) and Northwest University Scientific Research Foundation (No. 12NW24).

ORCID

Jun Li http://orcid.org/0000-0002-1474-6239

REFERENCES

[1] (a) S. Lipstman, *Crystal Growth and Design.* **2010**, *10*, 5001. (b) M. Shmilovits, D. P. Yael, I. Goldberg, *Crystal Growth and Design.* **2003**, *3*, 855.

[2] W. T. Chen, S. Fukuzumi, *Inorg. Chem.* **2011**, *50*, 671.

[3] C. C. Guo, W. J. Yang, Y. L. Mao, *J Mol Catal A-Chem.* **2005**, *226*, 279.

[4] R. D. Zorzi, N. Guidolin, S. Geremia, *J. Am. Chem. Soc.* **2009**, *131*, 2487.

[5] X. Xiao, W. J. Li, J. Z. Jiang, *Inorg. Chem. Commun.* **2013**, *35*, 156.

[6] A. Jasat, D. Dolphin, *Chem. Rev.* **1997**, *97*, 2267.

[7] C. M. Drain, A. Varotto, L. Radivojevic, *Chem. Rev.* **2009**, *109*, 1630.

[8] G. Rogez, C. Massobrio, P. Rabu, M. Drillon, *Chem. Soc. Rev.* **2011**, *40*, 1031.

[9] L. Ma, J. M. Falkowski, C. Abney, W. Lin, *Nat. Chem.* **2010**, *2*, 838.

[10] L. R. Fernandezde, M. K. Urtiaga, J. L. Mesa, E. S. Larrea, M. Iglesias, *Inorg. Chem.* **2013**, *52*, 2615.

[11] F. M. Arkaitz, B. Gotzone, I. A. María, B. Bazan, M. K. Urtiaga, E. S. Larrea, *Dalton Trans.* **2015**, *44*, 213.

[12] T. Zhang, W. B. Lin, *Chem. Soc. Rev.* **2014**, *43*, 5982.

[13] I. Beletskaya, V. S. Tyurin, A. Y. Tsivadze, R. Guilard, C. Stern, *Chem. Rev.* **2009**, *109*, 1659.

[14] N. A. Stephenson, A. T. Bell, *Inorg. Chem.* **2006**, *45*, 2758.

[15] Z. Q. Zhang, J. Li, Y. H. Yao, *Crystal Growth and Design.* **2015**, *15*, 5028.

[16] Y. J. Li, B. H. Sun, Y. R. Zhou, W. J. Yang, *Appl. Organomet. Chem.* **2016**, *31*, 1.

[17] A. Fateeva, P. Chater, C. P. Ireland, A. A. Tahir, Y. Z. Khimyak, P. V. Wiper, J. R. Darwent, M. J. Rosseinsky, *Angew Chem Int Ed.* **2012**, *51*, 7440.

[18] K. Peuntinger, T. Lazarides, D. Dafnomili, G. Charalambidis, G. Landrou, A. kahnt, R. Sabatini, D. McCamant, D. Gryko, *J. Phys. Chem. C* **2013**, *117*, 1647.

[19] J. T. Groves, T. E. Nemo, R. S. Myers, *J. Am. Chem. Soc.* **1979**, *101*, 1033.

[20] A. Dolbecq, E. Dumas, C. R. Mayer, P. Mialane, *Chem. Rev.* **2010**, *110*, 6009.

[21] J. Song, Z. Luo, C. L. Hill, D. K. Britt, H. Furukawa, O. M. Yaghi, K. I. Hardcastle, *J. Am. Chem. Soc.* **2011**, *133*, 16839.

[22] M. H. Xie, X. L. Yang, C. Zou, C. D. Wu, *Inorg. Chem.* **2011**, *50*, 5318.

[23] D. H. Lee, S. Kim, M. Y. Hyun, J. Y. Hong, S. Huh, C. Kim, S. J. Lee, *Chem Commun.* **2012**, *48*, 5512.

[24] M. H. Xie, X. L. Yang, C. D. Wu, Y. He, J. Zhang, B. Chen, *Chem. – Eur. J.* **2013**, *19*, 14316.

[25] X. S. Wang, M. Chrzanowski, C. Kim, W. Y. Gao, L. Wojtas, Y. S. Chen, X. P. Zhang, S. Q. Ma, *Chem Commun.* **2012**, *48*, 7173.

[26] D. Pogozhev, S. A. Baudron, M. W. Hosseini, *Inorg. Chem.* **2010**, *49*, 331.

[27] Y. X. Du, Z. Q. Zhang, J. Li, *Inorg. Chem. Commun.* **2016**, *64*, 19.

[28] G. M. Sheldrick, *SADABS, Program for Area Detector Adsorption Correction, Institute for Inorganic Chemistry*, University of Gottingen, Germany **1996**.

[29] G. M. Sheldrick, *SHELX-97 program for the solution of crystal structures*, University of Goettingen, Germany **1997**.

[30] Y. L. Zhang, C. Wang, X. Zhao, F. Yu, J. Li, *Inorg. Chem. Commun.* **2015**, *55*, 123.

[31] V. S. D. Silva, L. I. Teixeira, E. D. Nascimento, Y. M. Idemori, G. D. F. Silva, *Applied Catalysis A General.* **2014**, *469*, 124.

[32] W. Harhouri, S. Dhifaoui, Z. Denden, T. Roisnel, F. Blanchard, H. Nasri, *Polyhedron* **2017**, *130*, 127.

[33] X. L. Yang, M. H. Xie, C. Zou, C. D. Wu, *J. Am. Chem. Soc.* **2012**, *134*, 10638.

[34] Y. Yan, E. H. Kang, K. E. Yang, S. L. Tong, D. G. Famg, F. S. Xiao, *Catal. Commun.* **2004**, *5*, 387.

[35] L. Fu, Y. Chen, Z. Liu, *J Mol Catal A-Chem.* **2015**, *408*, 91.

SUPPORTING INFORMATION

Additional Supporting Information may be found online in the supporting information tab for this article.

How to cite this article: Yao Y, Du Y, Li J, Wang C, Zhang Z, Zhao X. Crystal structure of *meso*-substituted pyrazolyl porphyrin complexes and their highly active catalyst for oxidation of alkylbenzenes. *Appl Organometal Chem*. 2018;32: e4184. https://doi.org/10.1002/aoc.4184